https://doi.org/10.3311/PPci.19369

Periodica Polytechnica Civil Engineering, 66(2), pp. 367–383, 2022

Behavior of Square RC Short Columns with New Arrangement of Ties Subjected to Axial Load: Experimental and Numerical Studies

Hazem Elbakry[1], Tarek Ebeido[1], El-Tony M. El-Tony[1], Momen Ali[2*]

[1] Structural Engineering Department, Faculty of Engineering, Alexandrina University, Lotfy El- Sied St. off Gamal Abd El- Naser street, Alexandrina, Postal Code 21544, Egypt
[2] Construction Engineering and Management Department, Faculty of Engineering, Pharos University, Canal El-Mahmoudia street, Smouha, Alexandria, Postal Code 21311, Egypt
[*] Corresponding author, e-mail: momen.moharram@pua.edu.eg

Received: 07 October 2021, Accepted: 13 December 2021, Published online: 10 January 2022

Abstract

Reinforced concrete columns consume large quantities of ties, especially inner cross-ties in columns with large dimensions. In some cases, nesting of the pillars occurs as a result of the presence of cross-ties. The main objective of this paper is to develop new methods for transverse reinforcement in RC columns and investigate their effect on the behavior of the columns. The proposed V-ties as transverse reinforcement replacing the ordinary and cross-ties details are economically feasible. They facilitate shorter construction periods and decrease materials and labor costs. For this purpose, experimental and numerical studies are carried out. In the experimental program, nine reinforced concrete columns with identical concrete dimensions and longitudinal reinforcing bars were prepared and tested under concentric axial load with different tie configurations. The main parameters were the tie configurations and the length (l_v) of V-tie legs. As part of the numerical study, the finite element model using the ABAQUS software program obtained good agreement with the experimental results of specimens. A numerical parametric study was carried out to study the influence of concrete compressive strength and longitudinal reinforcement ratio on the behavior of RC columns with the considered tie configurations. Based on the experimental and numerical results, it was found that using V-tie techniques instead of traditional ties could increase the axial load capacity of columns, restrain early local buckling of the longitudinal reinforcing bars and improve the concrete core confinement of reinforced concrete columns.

Keywords

RC columns, transverse reinforcement, confinement effect, finite element analysis, concrete damage plasticity model, rebar buckling

1 Introduction

Reinforced concrete columns are considered one of the most important structural elements in different construction systems. They should, therefore, be studied to improve their behavior and performance. In the construction of RC columns, especially with large dimensions, one of the most important issues is the arrangement of transverse reinforcement as it consumes large quantities of ties, especially the inner ties. In some cases, nesting of the pillars occurs as a result of closed spaces of the cross-ties. The standard code requirements such as the American Concrete Institute [1] include the type of reinforcement used for ties, the quantity and the maximum distance between the transverse reinforcement. Middle bars are treated in the same manner as corner bars in order to prevent the buckling of longitudinal reinforcing bars.

Kim et al. [2] tested six rectangular solid section columns under cyclic lateral loads while being simultaneously subjected to constant axial loads. It was concluded that the proposed triangular reinforcement details might be an excellent alternative to conventional reinforcement details for easier, more reliable, and more rapid construction. The triangular confining reinforcement was also evaluated to ensure that longitudinal reinforcing buckling failure would not occur. Yang and Kim [3] tested fourteen RC columns to failure under a concentric axial load to examine the confinement effectiveness of the V-ties on the concrete core. It was concluded that the descending branch of the axial load-strain curve of columns dropped more rapidly in cross-ties columns than in the V-ties columns, which resulted in a higher ductility ratio in V-ties

Cite this article as: Elbakry, H., Ebeido, T., El-Tony, M. E.-T., Ali, M. "Behavior of Square RC Short Columns with New Arrangement of Ties Subjected to Axial Load: Experimental and Numerical Studies", Periodica Polytechnica Civil Engineering, 66(2), pp. 367–383, 2022. https://doi.org/10.3311/PPci.19369

columns than that in cross-ties columns. Beyond the ultimate strength of columns, 90-degree hooks of cross-ties were gradually opened, whereas no V-ties were extracted from concrete core during the period of tests, even for high-strength concrete columns. This resulted in a shorter buckling length of longitudinal reinforcement for V-ties columns than that for cross-ties columns.

Hwang et al. [4] tested five RC columns under compression concentric and eccentric loads. The test parameters were the shapes of transverse reinforcement (i.e., conventional cross-ties or U-tie bars), anchorage method of U-tie bars (i.e., straight bars or 90˚ hooked bars). Also, they tested ten reinforced concrete columns for cyclic load. The test parameters were the shape (i.e., conventional cross-ties or U-tie bars), anchorage method of U-tie bars replacing cross-ties (i.e., straight bars, 90˚ hooked bars, or headed bars), neutral axis depth of the column section (i.e., symmetric arrangement or asymmetric arrangement of longitudinal reinforcing bars), and cyclic loading conditions. In the compression test, the load carrying capacity and post peak behavior of the columns using U-tie bars for cross-ties were comparable to those of the column with conventional hoops and cross-ties. This result indicated that the U-ties can replace cross-ties and provide adequate lateral confinement. The results of the cyclic lateral load test showed that the structural capacity of the specimen was not significantly affected by the use of U-tie bars. This result indicated that when the shear demand was satisfied, U-tie bars could replace cross-ties.

Based on previous efforts by Watson et al. [5] and Sheikh et al. [6] on the behavior of concrete confined by transverse reinforcement, it was concluded that the stress-strain curves of confined concrete improved according to the quantities of transverse reinforcement.

As widely practiced Lukkunaprasit and Sittipunt [7] and Chung et al. [8], the ductility capacity of reinforced concrete columns could be improved by the confining force provided by transverse reinforcements.

2 Research significance

Most of the previous studies on the behavior of reinforced concrete columns have used deformed high-tensile reinforcement as transverse reinforcement and replaced the cross-ties with different shapes of transverse reinforcement. The commonly considered parameters in previous studies were the effect of anchorage method of different tie bars replacing cross-ties (i.e., straight bars, 90° hooked bars, or headed bars).

In this paper, some other parameters, which have not been studied by other researchers, are investigated. These parameters include using smooth mild steel bars as transverse reinforcement for V-ties, replacing outer conventional ties by individual V-ties for all longitudinal reinforcing bars including corner bars. This study presents an investigation on the approach of providing longitudinal reinforcing bars with V-ties, as an alternative method of traditional ties in order to facilitate quick installation and reduce the quantities of transverse reinforcement. Moreover, V-ties need no special workers and thus it contributes to the saving of both time and cost. For this purpose, experimental and numerical studies are carried out.

3 Experimental work program

In the experimental study, nine reinforced concrete columns with identical concrete dimensions and longitudinal reinforcing bars were prepared and tested under concentric axial load with different tie configurations. The specimens were divided into two groups according to the parameter being investigated as shown in Table 1.

Table 1 Test matrix

Group No.	Specimen	ρ_v, (%)	L_v, (mm)	Arrangement of Transverse Reinforcement at test zone	Characteristics
1	C	-	-	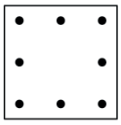	Without any ties
	CV-4	0.25	32		V-ties only for all longitudinal bars
	CV-10.5	0.53	85		
	CO	0.35	--	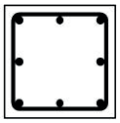	Outer traditional ties
	COC	0.6	--	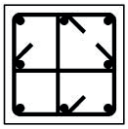	Outer traditional ties and cross-ties
2	COV-4	0.47	32		Outer traditional ties and V-ties for middle longitudinal bars
	COV-7	0.54	56		
	COV-10.5	0.61	85		
	COR	0.61	-	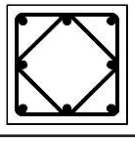	Outer traditional ties and rhombus ties

3.1 Details of tested columns

All specimens were constructed with the same concrete dimensions (1300 × 250 × 250 mm) and the same longitudinal reinforcing bars. The main parameters were the tie configurations and the length (l_v) of V-tie legs. Group 1 was reinforced with different outer tie configurations for all longitudinal reinforcing bars (no ties, V-ties and outer traditional ties). In group 2, transverse reinforcement was composed of outer traditional ties and different internal tie configurations for longitudinal middle reinforcing bars (cross ties, V-ties and rhombus ties). Two lengths of V-tie legs were considered; 32 mm and 85 mm in group (1). On the other hand, three lengths of V-tie legs were considered; 32 mm, 56 mm and 85 mm in group (2).

Group 1 consisted of four specimens. Column (C) was considered as a control specimen without any ties. Columns (CV-4 and CV-10.5) were reinforced by V-ties for all longitudinal reinforcing bars with different lengths of V-tie legs; 32 mm and 85 mm, respectively. Column (CO) was reinforced with outer traditional ties.

The second group consisted of five specimens. Column (COC) was reinforced by outer traditional ties and conventional cross-ties for middle longitudinal reinforcing bars. Columns (COV-4, COV-7 and COV-10.5) were reinforced by outer traditional ties and V-ties for middle longitudinal reinforcing bars with different lengths of V-tie legs; 32 mm, 56 mm and 85 mm, respectively. Column (COR) was reinforced with outer traditional ties and internal traditional rhombus ties.

The angle between the two legs of the V-tie bars was 45 degrees for all tested columns. The tested specimens had a square cross-section with a side length of 250 mm and the total height of the specimen was 1300 mm. The test region at mid-height of columns was 720 mm. The longitudinal reinforcing bars were 8Ø18 with reinforcement ratio of 3.26 % to emphasize the contribution of longitudinal reinforcing bars to the ultimate axial load capacity of specimens. The transverse reinforcement was made of smooth 8 mm diameter bars spaced at 240 mm. The wide spacing of the transverse reinforcement was chosen to increase the buckling length of longitudinal reinforcing bars in order to test the efficiency of the different tie configurations in supporting longitudinal reinforcing bars. The upper and lower stub regions of the columns had additional transverse reinforcement to avoid local failure. The clear concrete cover thickness, measured to the outer surface of the stirrups, was 20 mm.

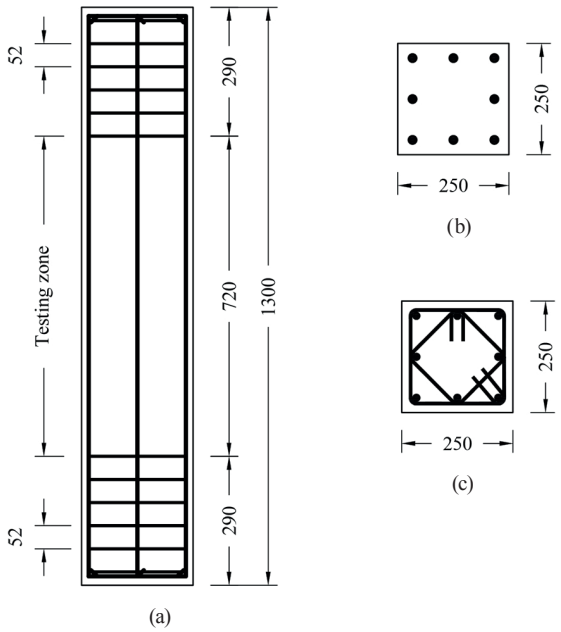

Fig. 1 Dimension and reinforcement details for control column C: (a) the longitudinal section; (b) cross-section at test zone; (c) cross section at upper and lower stub regions

Details of specimens are presented in Fig. 1 and Table 1. Figs. 2 and 3 show 3D views of longitudinal and transverse reinforcement used in groups 1 and 2, respectively. All specimens were cast horizontally in wooden forms. Standard concrete cubes (150 × 150 × 150 mm) were also cast with the column specimens. Two days after casting, the standard cubes and the sides of the specimens were stripped from the molds and covered with wet burlap for seven days. After that, the burlap was removed and the specimens were allowed to air-dry until testing.

3.2 Material properties

The concrete mix contained a blend of pink crushed limestone as the coarse aggregate having a maximum aggregate size of 10 mm and sand with a maximum size of 4.75 mm. The used cement was Ordinary Portland Cement (OPC) as the main binder. The mix proportions for one cubic meter of mixed concrete are listed in Table 2. The average compressive cube strength was 25 MPa measured on the day of the specimen test. It was measured using three standard concrete cubes (150 × 150 × 150 mm) for each specimen. The standard cubes were subjected to the same curing conditions of the tested specimens. To determine the mechanical properties of reinforcing bars, tensile tests were performed on three specimens for each bar size. The average nominal yield stress of the used longitudinal reinforcing

(a) (b) (c)

Fig. 2 3D view showing the different configurations of outer ties used in group 1: (a) without any tie control column C; (b) V-ties for all longitudinal reinforcing bars specimens CV-4 and CV-10.5; (c) outer traditional tie specimen CO

(a) (b) (c)

Fig. 3 3D view showing the different configurations of internal ties used in group 2: (a) outer tie and traditional cross-ties specimen COC; (b) outer tie and V-ties for middle longitudinal bars only specimens COV-4, COV-7 and CV-10.5; (c) outer tie and rhombus internal tie specimen COR

Table 2 Concrete mix proportions/m^3

Cement	Sand	Gravel	Water/Cement
333 Kg	667 Kg	1167 Kg	0.6

bars of 18 mm diameter was 480 MPa. The used stirrups were made of smooth mild steel bars of 8 mm diameter with average nominal yield stress 320 MPa. The mean values of the mechanical properties of the longitudinal and transverse reinforcing bars are summarized in Table 3.

- For group 1, Specimen notation includes three parts. The first letter refers to reinforced concrete columns C. The second letter gives arrangement of ties: V for V-ties and O for traditional outer ties. The third is used to identify extension length of V-tie legs. For example, Specimen CV-10.5 indicates column having V-ties arrangement and V-ties with extension length of V-tie legs 10.5 φ_s. On the other hand, Specimen notation includes four parts in group 2. The first letter refers to reinforced concrete columns C. The Second letter gives outer ties. The third is used to identify type of internal transverse reinforcement: C for cross-tie, V for V-ties, and R for rhombus ties. The fourth is used to identify extension length of V-tie legs. For example, Specimen COV-7 indicates column having a traditional ties as outer transverse reinforcement and V-ties with extension length of V-tie legs 7 φ_s as internal transverse reinforcement for middle bars only.
- φ_s and ρ_v are diameter and volumetric ratio of transverse reinforcement, l_v is extension length of V-tie legs into concrete core.

Table 3 Mechanical properties of steel bars

Diameter of steel bar, mm	Type	Average yield stress, MPa	Average tensile strength, MPa	Average modulus of elasticity, GPa	Elongation, %
18	Deformed high-tensile steel	480	601	203	25
8	Smooth mild steel	320	472	201	30.4

3.3 Test setup and instrumentation

All specimens were tested on a test setup as shown in Fig. 4(a). All columns were concentrically loaded using a 3,000 kN capacity universal compression machine. Load was incrementally applied to the specimen at an average rate of 150 kN/min. The specimens were tested under concentric axial load by applying the load on three-dimensional steel spreader caps at columns ends. The overall dimensions of the caps were 280 × 280 × 100 mm and they were made of 30 mm thick plates which distribute the column compression load at the ends. For all specimens, four strain gauges were placed on mid-height of longitudinal reinforcing bars at the four corners of specimen to measure the vertical strains. The positions of four strain gauges for all tested specimens are shown in Fig. 4(b). The loading continued until the specimen failure. After each loading step, the acting loads on the specimen and the strain gauges' readings were recorded and stored using a data logger.

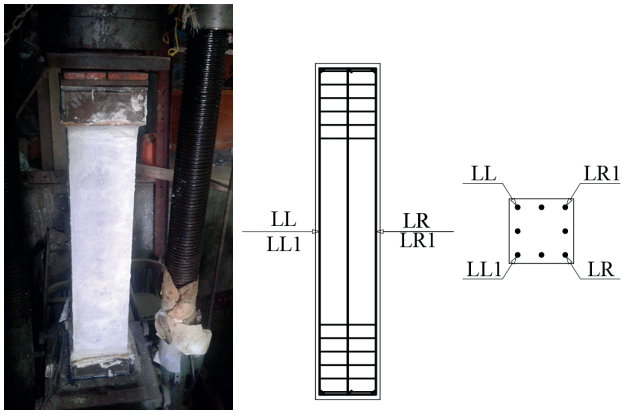

(a) (b)

Fig. 4 Test setup and instrumentation: (a) Test setup; (b) Locations of strain gauges

4 Experimental results

All columns had been tested up to complete failure. Table 4 summarizes the experimental results for all tested columns. In addition, further discussion on the mode of failure and the ultimate axial load for all tested columns are presented and compared herein below.

4.1 Failure modes

Fig. 5 shows the shape of failure of tested columns in group 1. It indicated that the damage scheme to the specimens was buckling of the longitudinal reinforcing bars, spalling of the concrete cover and failure of the concrete core. This type of failure may have been triggered by the buckling of the longitudinal bars which resulted in spalling of the concrete cover and was promptly followed by the failure of the concrete core. After buckling of the longitudinal reinforcing bars and concrete spalling was observed, the recorded applied load decreased rapidly. Fig. 6 shows the mode of failure for specimens in group 2. The effectiveness of V-ties to prevent the buckling of corner longitudinal bars when replacing outer traditional ties for specimen CV-10.5 is displayed in the photo of the specimen after failure in Fig. 7(a). Fig. 7(b) shows the effect of V-ties, as internal transverse reinforcement replacing cross-ties, on restraining the buckling of middle longitudinal reinforcing bars for specimen COV-10.5.

4.2 Ultimate loads

Table 4 shows experimental ultimate axial loads of the all tested columns in groups 1 and 2. It could be noted that the highest ultimate capacity was exhibited by specimen COR, while the lowest ultimate capacity was achieved by column C which had no ties. Table 4 shows the percentage of increase in the ultimate axial load for all tested columns

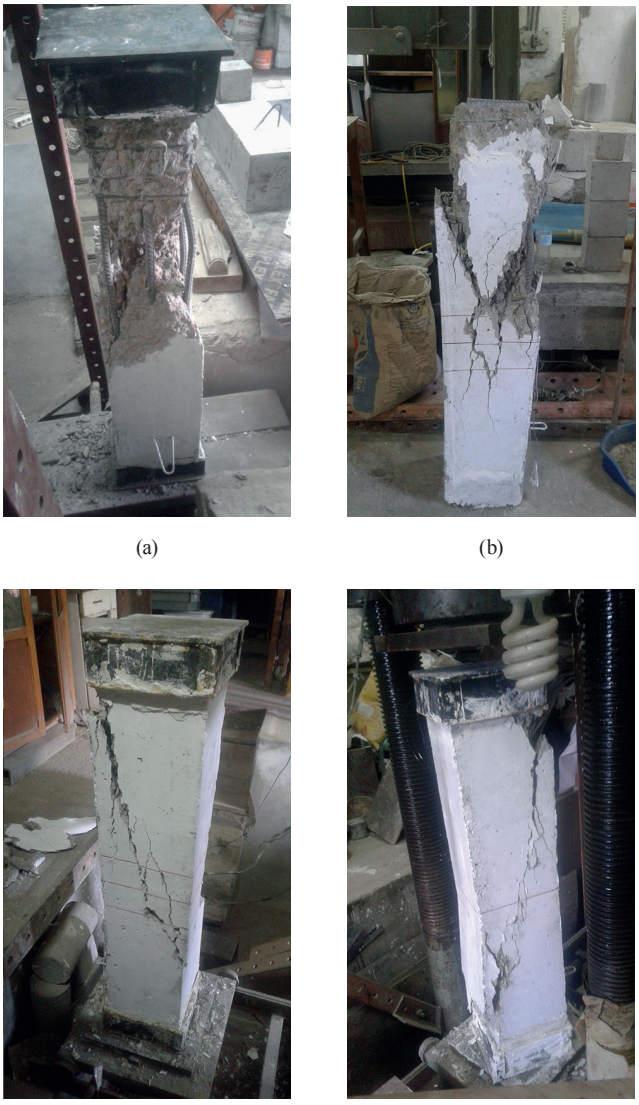

(a) (b) (c) (d)

Fig. 5 Modes of failure for specimens in group 1; (a) C, (b) CV-4, (c) CV-10.5, (d) CO

compared to that of the control column C. The table also shows the relationships between ultimate axial loads of all tested specimens and the nominal axial load obtained from Eq. (1) as proposed by ACI 318-19 [1].

The nominal axial capacity of the column cross-section based on Eq. (1), as recommended by ACI 318-19 [1], was about 2007 KN.

$$P_o = 0.85 f_c^{'} \left(A_C - A_s \right) + A_s f_y \,, \tag{1}$$

where P_o is the nominal axial capacity of the column cross-section; f_c' is concrete cylinder compressive strength (MPa); f_y is yield stress of the longitudinal reinforcing bars (MPa); A_c is concrete cross-sectional area (mm^2); and A_s is the total cross-sectional area of the longitudinal reinforcing bars (mm^2).

(a) (b) (c) (d) (e)

Fig. 6 Modes of failure for tested columns in group 2; (a) COC, (b) COV-4, (c) COV-7, (d) COV 10.5, (e) COR

(a) (b)

Fig. 7 Effectiveness of V- ties in preventing the buckling of longitudinal reinforcing bars: (a) corner longitudinal bars specimen CV-10.5; (b) middle longitudinal bars specimen COV-10.5

Table 4 Experimental results versus axial load capacity obtained of ACI 318-19

Specimen	$(P_u)_{Exp}$ (kN)	More $(P_u)_{Exp}$ Vs. col. C (kN)	More $(P_u)_{Exp}$ Vs. col. C (%)	$(P_u)_{Exp}$ / $(P_u)_{ACI}$	Wt. of one tie (kg)	More $(P_u)_{Exp}$/ weight of tie (kN/kg)
C	1970	--	--	0.98	--	--
CV-4	2190	220	11.16	1.09	0.29	759
CV-10.5	2260	290	14.72	1.13	0.63	460
CO	2240	270	13.70	1.12	0.41	659
COC	2360	390	19.79	1.17	0.71	549
COV-4	2300	330	16.75	1.15	0.56	589
COV-7	2350	380	19.28	1.17	0.63	603
COV-10.5	2400	430	21.82	1.20	0.72	597
COR	2460	490	24.87	1.23	0.72	681

Fig. 8 shows the ultimate axial loads of specimens in group 1. Columns CV-4, CV-10.5, and CO achieved an increase in ultimate axial load of 11.2%, 14.7% and 13.7%, respectively, compared to that of the control column C. It was observed that specimen CV-10.5 recorded the highest increase in ultimate load 14.7% compared to specimen C. This proved that V-ties had a significant effect on ultimate load capacity by preventing buckling of longitudinal reinforcing bars and made good confinement of concrete core. It could be noted that specimen CV-10.5 achieved an increase in ultimate load of 3.6% compared with specimen CV-4. This showed that increasing the length of V-tie legs from 32 to 85 mm had a slight effect on ultimate load.

The experimental ultimate axial load of column C was 1970 kN which was close to the value of axial load obtained from ACI 318-19 [1] Eq. (1). The ultimate axial loads of columns CV-4, CV-10.5, and CO achieved an increase in ultimate load capacity of 9%, 13%, and 12%, respectively, compared to the nominal load obtained from ACI 318-19 [1] Eq. (1).

The ultimate axial loads of tested specimens in group 2 are shown in Fig. 9. Specimens COC, COV-4, COV-7, COV-10.5 and COR achieved an increase in ultimate axial load capacity by 19.8%, 16.8%, 19.3%, 21.8% and 24.9%, respectively, compared with specimen C. It was observed that adding internal transverse reinforcement increased the ultimate load capacity by ratios ranging from 2.7% to 9.8% compared to specimen CO with outer traditional ties only. This indicated the importance of internal transverse reinforcement to prevent buckling of middle longitudinal bars and to enhance the concrete core confinement of reinforced concrete columns and, consequently, increase the ultimate axial load. The ultimate loads of specimens

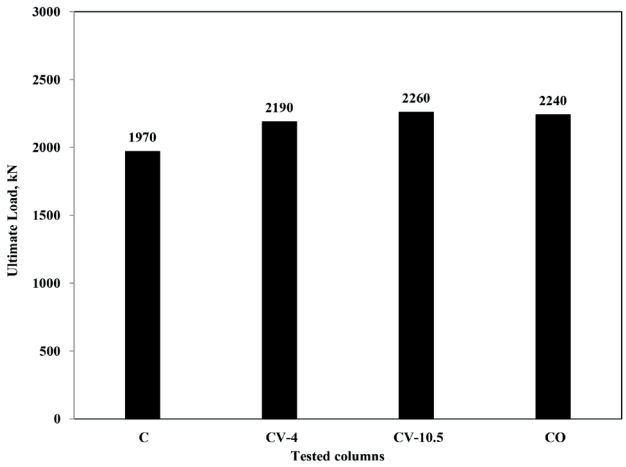

Fig. 8 Axial loads for specimens in group 1

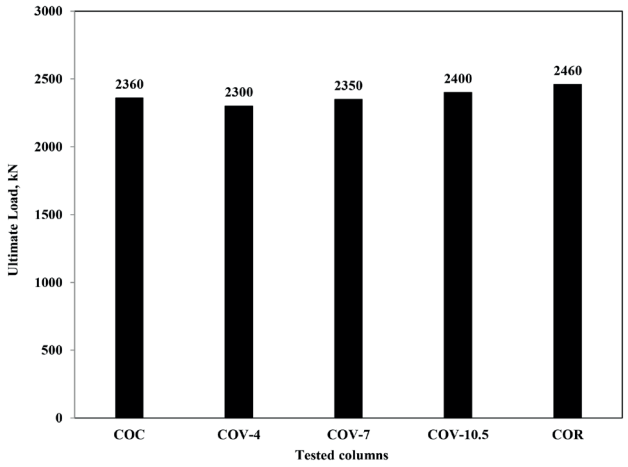

Fig. 9 Axial loads for specimens in group 2

COV-4, COV-7, and COV-10.5 achieved an increase in ultimate load capacity of 2.7%, 4.9% and 7.1%, respectively, compared to that of specimen CO. It could be concluded that the effect of V-ties, as internal transverse reinforcement, on increasing the ultimate axial load capacity of RC columns is significant.

It was observed that specimen COV-10.5 achieved an increase in ultimate load capacity of 4.5% and 2.2% compared with specimens COV-4 and COV-7, respectively. This indicated that the extension of V-tie legs in concrete core had a significant effect on the ultimate load by restraining buckling of middle longitudinal reinforcing bars and improving confinement of concrete core.

To study the effect of using V-ties for corner longitudinal bars instead of traditional square ties, specimens CV-4 and CV-10.5 were compared with specimens COV-4 and COV-10.5, respectively. The ultimate load capacity of specimen CV-4 was 4.8% lower than that of specimen COV-4. Similarly, the ultimate load capacity of specimen CV-10.5 was 5.8% lower than that of specimen COV-10.5. This showed that using V-ties for the outer longitudinal bars did not provide the same restraining and confining effect of the square traditional ties.

To study the effect of using V-ties for middle longitudinal bars instead of traditional cross-ties, specimens COV-4, COV-7 and COV-10.5 were compared with specimen COC. The ultimate load capacity of specimens COV-4 and COV-7 were 2.5% and 0.4% lower than that of specimen COC. On the other hand, the ultimate load capacity of specimen COV-10.5 was 1.7% higher than that of specimen COC. This showed that using V-ties for the middle longitudinal bars with 56 mm leg length had almost the same axial ultimate load of traditional cross-ties and that the V-ties could outperform cross-ties particularly for V-ties with 85 mm leg length.

To study the effect of using V-ties for middle longitudinal bars instead of traditional rhombus ties, specimens COV-4, COV-7 and CV-10.5 were compared with specimen COR. The ultimate load capacity of specimens COV-4, COV-7 and COV-10.5 were 6.5%, 4.5% and 2.4% lower than that of specimen COR. It could be concluded that using V-ties for the middle longitudinal bars was slightly less effective than traditional rhombus ties as far as the ultimate axial load capacity of RC columns was concerned.

The ultimate axial loads of columns COC, COV-4, COV-7, COV-10.5 and COR achieved an increase in ultimate axial load capacity of 17%, 15%, 17%, 20% and 23%, respectively, compared to the nominal axial load obtained from ACI 318-19 [1] Eq. (1).

4.3 Axial strains

Fig. 10 shows the relationships between the acting axial load and axial strain for tested specimens in group 1. The axial strains were calculated as the average strain obtained

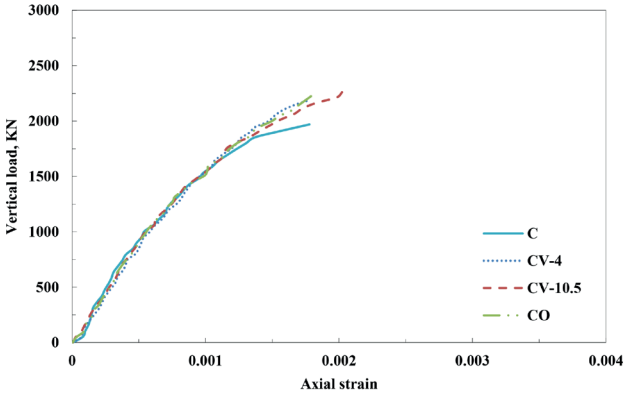

Fig. 10 Axial loads and axial strain relationships for columns in group 1

from the four strains on the longitudinal reinforcing bars at the corners of specimens. It could be observed that all specimens had almost the same stiffness through early phases of the test. This showed that the effect of ties on the initial stiffness of tested specimens was insignificant. It could also be observed that CV-4, CV-10.5 specimens and CO had almost the same stiffness through the last phase of the test which was generally higher than that of specimen C. This indicated that the V-ties, in general, improved the stiffness of specimens in a similar manner as the outer traditional ties did. It could be concluded that the V-ties with short leg length had achieved approximately the same behavior as both the V-ties with long leg length and ordinary outer ties.

Fig. 11 shows the axial strain curves of all tested columns in group 2. It could be observed that all specimens had almost the same behavior, especially through early phases of loading. This indicated that different internal tie configurations had almost the same effect on the initial stiffness of all tested specimens. At the final phase of loading, however, specimen COR, with internal rhombus ties, had slightly higher stiffness compared with other specimens in group 2. Specimens with both V-ties and cross ties still had almost the same behavior. This showed that the replacement of traditional ties with V-ties technique is practically effective and economic.

The relationships between axial load and axial strain of all tested specimens in groups 1 and 2 are shown in Fig. 12. It was generally observed that the internal transverse reinforcement increased the stiffness of RC columns, especially at the final phases of loading, compared with specimens with outer transverse reinforcement only.

4.4 Cost–benefit analysis

On performing a cost-benefit analysis, the quantities of only the transverse reinforcement were considered and compared. The cost of formation and operation was assumed to be constant for all types of reinforcement. In comparing the strength of the specimens, the strength gain, which was the increase in specimen strength compared to specimen C, was used instead of the total strength as shown in Table 4. This was adopted to focus on the effect of transverse reinforcement on the column strength and exclude the contributions of the concrete section and longitudinal reinforcement. The weight of one tie for each of the considered configurations is also shown in Table 4.

For specimens in group 1, it was concluded that specimen CV-4 recorded a cost reduction of ties by 30% compared to specimen CO and this was associated with only

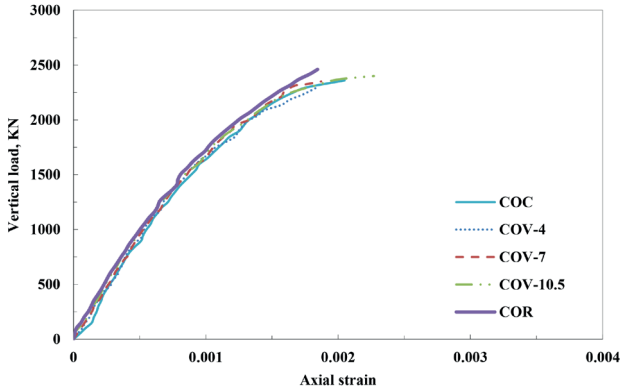

Fig. 11 Axial loads and axial strain relationships for columns in group 2

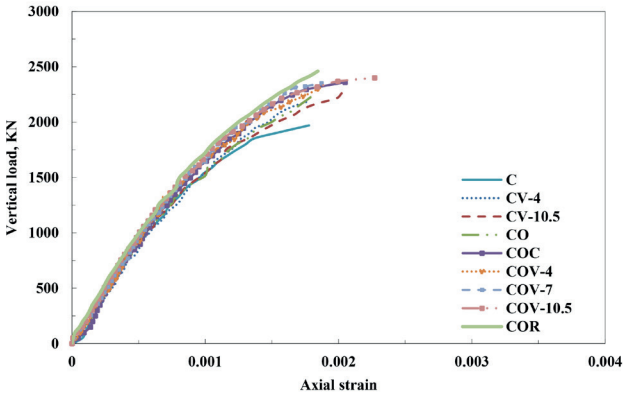

Fig. 12 Axial loads versus axial strain relationships for columns in groups 1 and 2

a 19% reduction of strength gain. On the other hand, CV-10.5 recorded a cost increase of ties by 46% compared to specimen CO and this was associated with a 7% increase of strength gain. Furthermore, specimen CV-10.5 recorded a cost increase of ties by 111% compared to specimen CV-4 and this corresponded to a 32% increase of strength gain. This showed that the use of V-ties instead of outer traditional ties was economically feasible.

In group 2, it was found that specimens COC and COR recorded a cost increase of ties of 61% and 69% compared to specimen CO and this was associated with 44% and 81% increase of strength gain, respectively. This showed that the rhombus ties were more efficient than the cross ties. Specimens COV-4, COV-7 and COV-10.5 recorded a cost increase of ties of 31%, 46% and 69% compared to specimen CO and this was associated with 22%, 41% and 59% increase of strength gain, respectively. This showed that the use of V-ties instead of inner traditional ties was economically feasible.

To quantify the effectiveness of the different configurations of the transverse reinforcement, the gain in column strength due to the effect of transverse reinforcement per

unit weight of the corresponding ties was calculated for each specimen (in kN/kg). The weight of the ties was calculated for one tie for each configuration which was considered sufficient for comparison purposes. The gain in column strength per unit weight of ties is shown in Table 4 which could be termed as the specific gain.

For specimens of group 1, with V-ties for all bars, it was found that the most effective configuration was that of specimen CV-4 with a specific gain of 759 kN/kg. For specimen CO, with outer traditional ties, the specific gain was 659 kN/kg. This shows that V-ties with leg length of 32 mm outperformed the traditional square ties as far as the effectiveness of the used material. Specimen CV-10.5, having V-ties with leg length of 85 mm, had the least specific gain of 460 kN/kg.

For specimens of group 2, with a traditional square outer tie and different configurations of ties for internal bars, it was found that the most effective configuration was that of specimen COR with a specific gain of 681 kN/kg. Specimens COV-4, COV-7 and COV-10.5 had lower specific gains of 589 kN/kg, 603 kN/kg and 597 kN/kg, respectively. Out of the specimens with V-ties for the internal bars, specimen COV-7 had the highest specific gain. The least effective configuration was the cross ties of specimen COC with a specific gain of 549 kN/kg. This showed that V-ties are generally effective and could be more economical than some of the traditional ties.

5 Numerical analysis

To extend the results obtained in the experimental study, a nonlinear Finite Element (FE) analysis was conducted using the commercially available finite element analysis package Abaqus/standard [9]. The main objective of the numerical study was to adopt an FE model to predict the general behavior of reinforced concrete columns subjected to concentric axial load taking into consideration the effect of transverse reinforcement. A brief description of the constitutive models that were used is described below.

5.1 Material properties and constitutive models

In the current paper, the concrete was modeled using 4-node linear tetrahedron solid element (C3D4) with three displacement degrees of freedom for each node. Steel reinforcing bars was modeled using 3-D, 2-node truss elements with three degrees of freedom at each node. The bond between steel reinforcing bars and concrete was assumed to be a perfect bond. To simulate the experimental setup two steel plates with dimensions (250 × 250 × 60 mm) are identified with an elastic-plastic behavior assigned. A rigid plate at each end of the RC column is used to assure a uniform distribution of the axially applied load. Such a rigid plate can prevent the local failure of concrete due to stress concentration at the column ends. Load control method is adopted to determine the column capacity and post-cracking behavior of the RC columns. For this study, different mesh sizes were tried to reach the optimum size for the FEM modeling. Mesh convergence starts from fine meshes to a fairly coarse mesh. The considered mesh element sizes were 25 mm, 30 mm, 50 mm, 75 mm and 100 mm. Fig. 13 shows the results obtained for element sizes ranging from 25 mm to 100 mm for specimen CO. The results showed that the optimum size was 30 mm which gave the best results compared with both other sizes and experimental results.

5.1.1 Concrete material

In the current study, the concrete damage plasticity model (CDP) was used to model the concrete behavior. CDP allows for separate strain rates, yield strengths and damages parameters in compression and tension.

The elastic parameters required to establish the tension stress-strain curve are elastic modulus, E_c, and tensile strength, f_{ct}. According to ACI 318-19 [1] E_c and f_{ct} were calculated by:

$$E_c = 4700\sqrt{f_c'}\,, \tag{2}$$

$$f_{ct} = 0.33\sqrt{f_c'}\,, \tag{3}$$

where; f_c' is the cylinder compressive strength of concrete.

Five main parameters were considered for the concrete model; the yield surface shape K_c, the eccentricity Є, the stress ratio σ_{bo}/σ_{co}, the viscosity regularization υ and the dilation angle ψ. The CDP model considers the non-associated

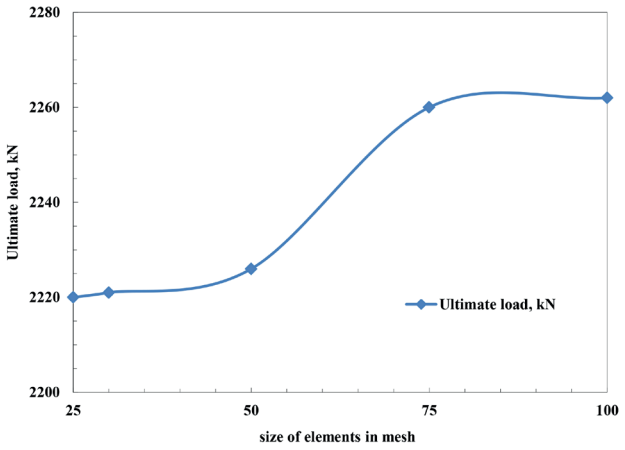

Fig. 13 Mesh convergence study for specimen CO

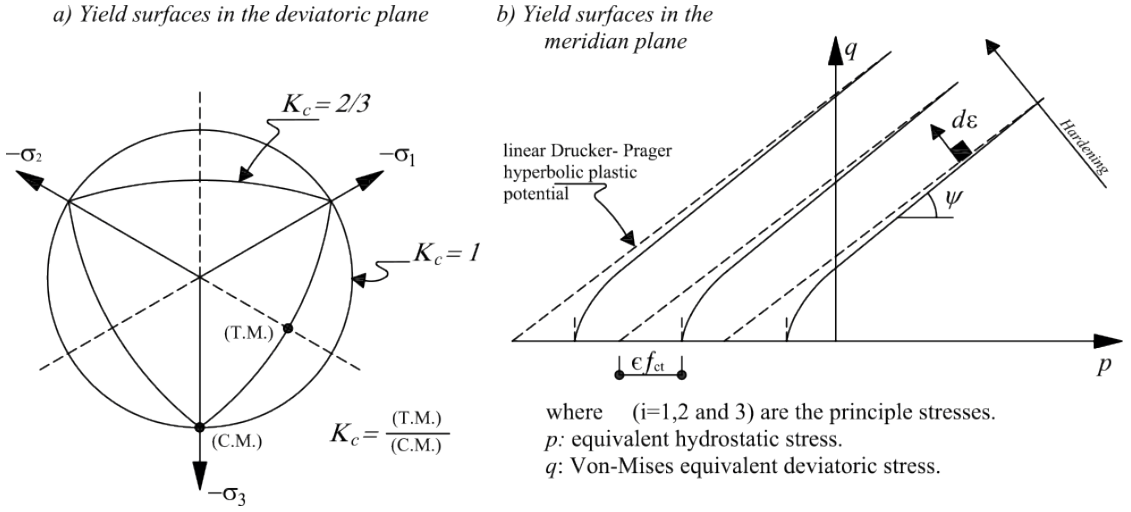

Fig. 14 CDP model yield surface and its parameters ψ, ϵ, and K_c [18, 19]

Drucker-Prager hyperbolic flow potential function $G(\sigma)$, as in, [1, 9–13] see Fig. 14. The parameter K_c, shown in Fig. 14(a) represents the ratio between the tension meridian and compression meridian in the deviatoric cross section. ABAQUS [9] considers the default value for K_c to be equal to 0.667. ϵ is a small positive dimensionless value, known as the flow potential eccentricity, which defines the rate at which the function $G(r)$ approaches the asymptote presented in a dashed line in Fig. 14(b). ABAQUS [9] recommends a default value of ϵ equal to 0.1. The CDP model accounts for the parameter σ_{bo}/σ_{co} which is the ratio of the equal biaxial compressive strength σ_{bo} to the uniaxial compressive strength σ_{co} (i.e., $\sigma_{co}=f_c$). The default value recommended in ABAQUS [9] σ_{bo}/σ_{co} is equal to 1.16. For the viscosity υ parameter, ABAQUS [9] recommends a default value equal to 0. Many experimental and numerical studies were collected from literature to calibrate dilation angle ψ parameter. The optimum dilation angle was 38° according to Ali et al. [14]. Table 5 provides the values of the CDP model parameters considered in default values in ABAQUS [9] except for the dilation angle which was obtained from literature.

There are different forms of tension stiffening models; the model developed by Wahalathantri et al. [15] was selected for the present study as it is applicable for the reinforced concrete member. Moreover, this method indicates similarity to the tension stiffening model that is needed for concrete damaged plasticity model CDP. This tension stiffening model was originally based on the homogenized stress-strain relationship developed by Nayal and Rasheed [16] which accounts for tension softening. Fig. 15 shows the modified tension stiffening model for ABAQUS [9].

Table 5 Values of CDP model parameters

Item	ψ	ϵ	K_c	σ_{bo}/σ_{co}	υ
Parameter value	38°	0.1	0.667	1.16	0.0

ψ = the dilation angle, ϵ = the eccentricity, K_c = yield surface shape, σ_{bo}/σ_{co} = the stress ratio, υ = the viscosity regularization

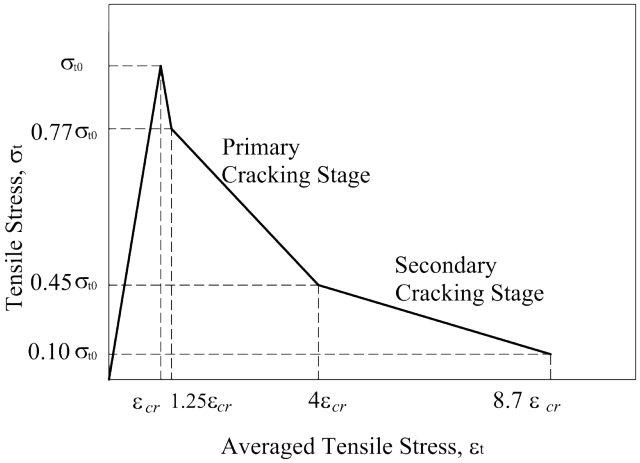

Fig. 15 Modified Tension Stiffening Model for ABAQUS [9]

For the compression stress-strain curve of the concrete, the stress–strain relationship proposed by Desayi and Krishnan [17] was used to construct the uniaxial compressive stress–strain curve. Equations (4) to (7) were used to construct the uniaxial compressive stress–strain curve for concrete. Typical compressive stress-strain relationship with damage properties and terms are illustrated in Fig. 16.

$$\sigma_c = \frac{E_c \varepsilon_c}{1+\left(R+R_E-2\right)\left(\frac{\varepsilon_c}{\varepsilon_o}\right)-\left(2R-1\right)\left(\frac{\varepsilon_c}{\varepsilon_o}\right)^2+R\left(\frac{\varepsilon_c}{\varepsilon_o}\right)^3}, \quad (4)$$

where σ_c is the compressive stress at any ε_c, ε_c is the effective strain; ε_o is strain at the ultimate stress.

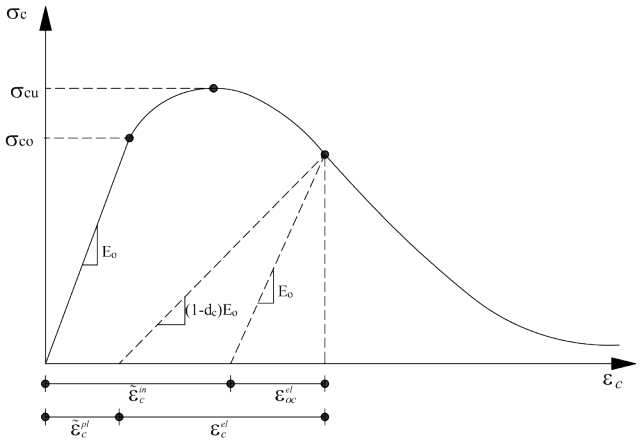

Fig. 16 Terms for concrete compressive stress-strain relationship ABAQUS Manual [9]

$$R = \frac{R_E\left(R_\sigma - 1\right)}{\left(R_\varepsilon - 1\right)^2} - \frac{1}{R_\varepsilon}, \tag{5}$$

$$R_E = \frac{E_c}{E_o}, \tag{6}$$

$$E_o = \frac{f_c}{\varepsilon_o}, \tag{7}$$

where R is the material parameter depending on the shape of the stress-strain curve, E_o is the initial undamaged elastic stiffness of the material, (f_c) is the cylinder compressive strength, $R_\varepsilon = 4$, $R = 4$ as reported by Hu and Schnobrich [20]. Poisson's ratio for concrete was assumed to be 0.20.

5.1.2 Steel reinforcement

The behavior of reinforcing steel bars was assumed to be as a bilinear elastic-plastic material and identical in tension and compression. The plastic Young's modulus was assumed as 0.1 E_s. The elastic modulus E_s, the yield stress σ_y, and the ultimate stress σ_u are shown in the Table 3. Poisson's ratio of 0.3 was used for the steel reinforcing bars according to Sakr et al. [21].

6 Comparison of experimental and finite element results

The FE analysis was carried out on nine RC numerical models representing the RC columns tested in the present experimental program. Table 1 gives the properties of columns analyzed using the FE program ABAQUS [9]. The specimens were 1300 mm in height and had a square section of 250 mm side length. The actual material properties that were obtained from experimental results were considered in the analysis. Comparison of numerical and experimental results shows that the model can satisfactorily represent behavior of RC columns with the CDP model under axial concentric load. Both detailed and global analyses were successfully performed using the developed model. The experimental and numerical results of specimens C, CV-4, CV-10.5, and CO are plotted in Figs. 17–20, respectively. The load-strain curves obtained from experimental and numerical studies for specimens COC, COV-4, COV-7, COV-10.5, and COR are shown in Figs. 21–25, respectively. It can be observed that the numerical results obtained using the proposed CDP model can provide a fair

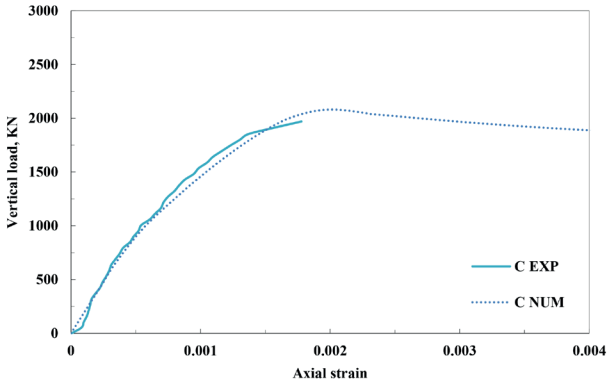

Fig. 17 Load-strain curve obtained from experimental and numerical studies for specimen C

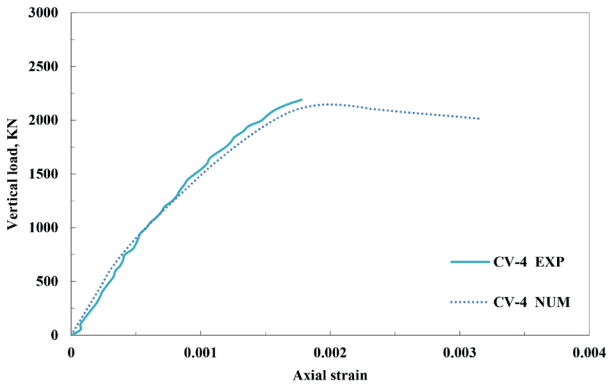

Fig. 18 Load-strain curve obtained from experimental and numerical studies of column CV-4

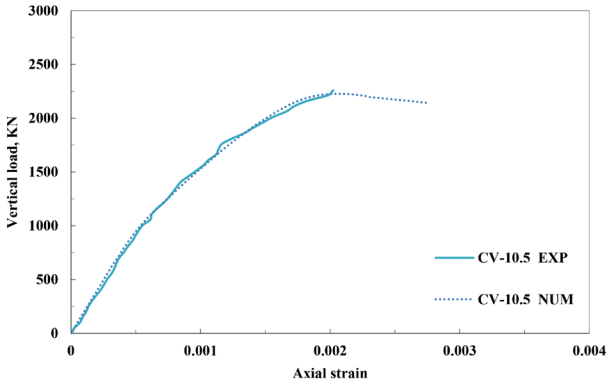

Fig. 19 Comparison of the load-strain curve obtained from experimental and numerical studies of specimen CV-10.5

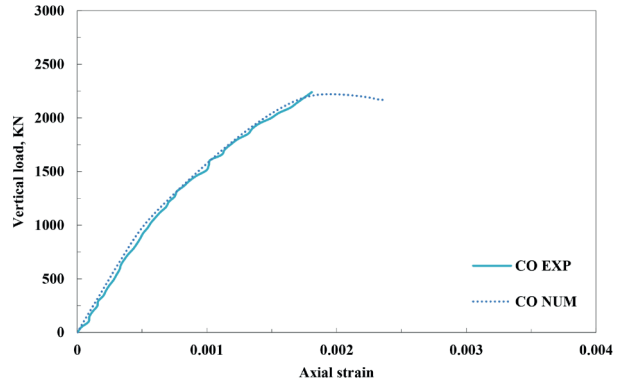

Fig. 20 Comparison of the load-strain curve obtained from experimental and numerical studies of column CO

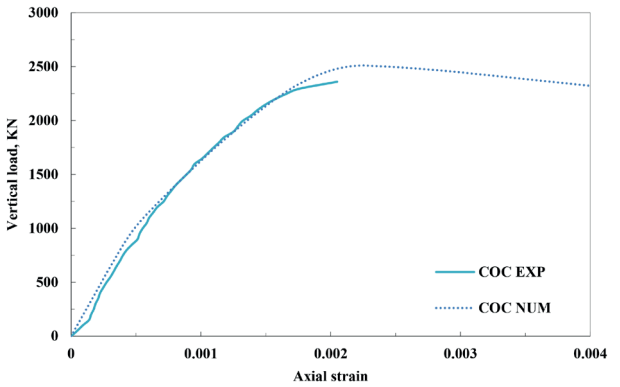

Fig.21 Comparison of the load-strain curve obtained from experimental and numerical studies of specimen COC

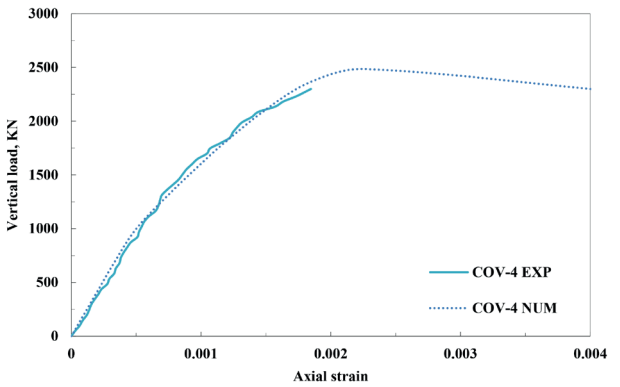

Fig. 22 Comparison of the load-strain curve obtained from experimental and numerical studies of specimen COV-4

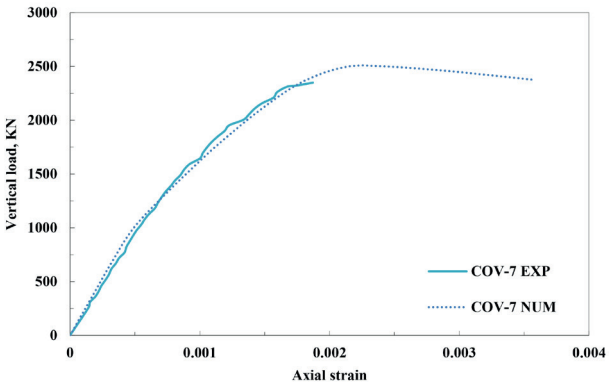

Fig. 23 Load-strain curve obtained from experimental and numerical studies for specimen COV-7

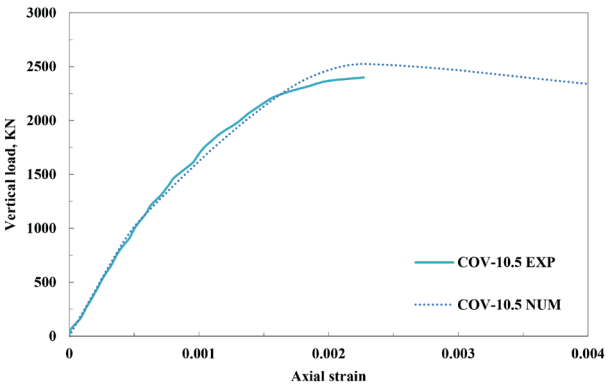

Fig. 24 Comparison of the load-strain curve obtained from experimental and numerical studies of specimen COV-10.5

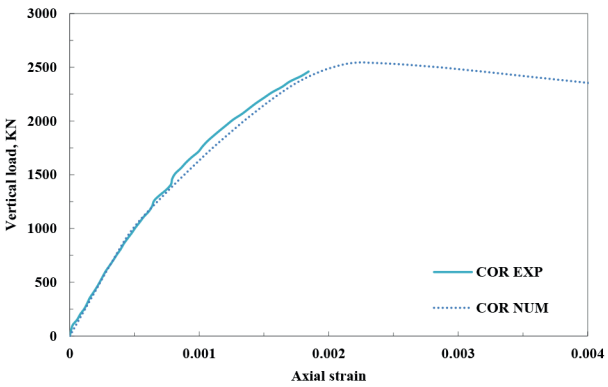

Fig. 25 Comparison of the load-strain curve obtained from experimental and numerical studies for column COR

agreement with the experimental results for all tested columns. However, slight deviations occurred in the $(P_u - \varepsilon_c)$ curve. The experimental and numerical ultimate axial loads recorded by all the specimens are shown in Table 6. The maximum deviation from the experimental results at peak loadings was approximately 8 %. Figs. 26 and 27 show the experimental and numerical ultimate axial loads for all specimens in groups 1 and 2, respectively. Modes of failure of both cases of V-ties for all longitudinal reinforcing bars specimen (CV-10.5), and V-ties for middle longitudinal reinforcing bars specimen (COV-10.5) obtained from experimental and numerical studies are shown in Figs. 28 and 29, respectively. Based on these figures, it was clear that the comparison was very satisfactory indicating significant matching between the experimental and numerical studies.

7 Parametric studies

A parametric study was conducted by using the finite element model. The study focused on the most important parameters that can affect the behavior of RC columns such as the strength of concrete and the longitudinal reinforcing ratio. In each analysis, only one variable is changed at a time, while keeping all other parameters constant during the analysis.

Table 6 Numerical axial loads and comparison with experimental results of the tested columns

Group No.	Specimen	$(P_u)_{Exp}$ (kN)	$(P_u)_{Num}$ (kN)	$(P_u)_{Exp}/(P_u)_{Num}$
1	C	1970	2081	0.95
	CV-4	2190	2147	1.02
	CV-10.5	2260	2227	1.01
	CO	2240	2221	1.01
2	COC	2360	2511	0.94
	COV-4	2300	2487	0.92
	COV-7	2350	2510	0.94
	COV-10.5	2400	2526	0.95
	COR	2460	2545	0.97

$(P_u)_{Exp}$ is ultimate load obtained from experimental results;
$(P_u)_{Num}$ is ultimate load obtained from numerical results

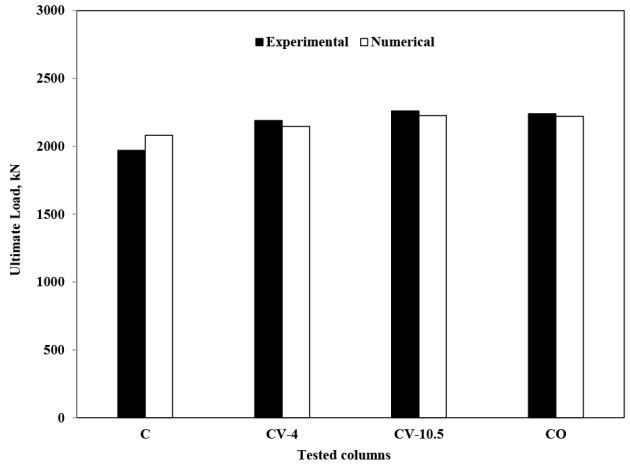

Fig. 26 Comparison of the ultimate axial loads obtained from experimental and numerical studies of group 1

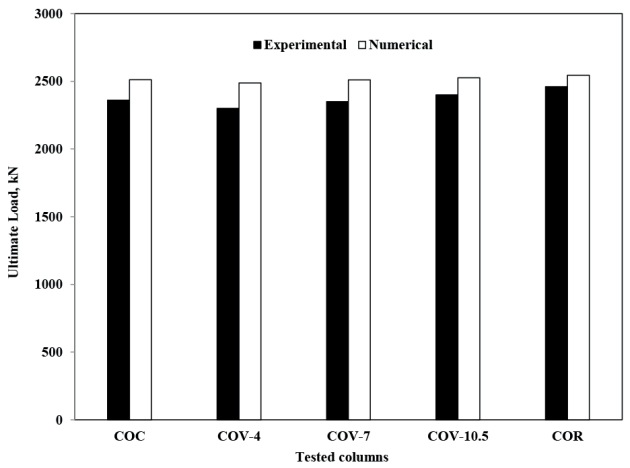

Fig. 27 Comparison of the ultimate axial loads obtained from experimental and numerical studies of group 2

7.1 Concrete compressive strength

The effect of concrete compressive strength was studied by modeling all columns. For each column, the concrete cube compressive strength values of 25, 35 and 45 MPa were considered at different values of longitudinal reinforcing ratio 3.26%, 2.57% and 1.45%.

Fig. 30 shows the influence of concrete strength on the ultimate load of RC columns for all specimens at longitudinal reinforcing ratio 3.26%. It can be seen that, the ultimate axial loads of RC columns increased linearly by the increase in concrete grade.

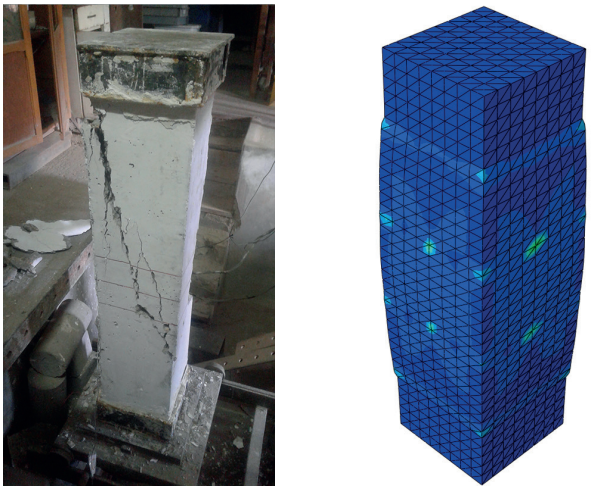

(a) (b)

Fig. 28 Modes of failure and crack survey for specimen CV-10.5: (a) experimental damage; (b) FE model plastic strain

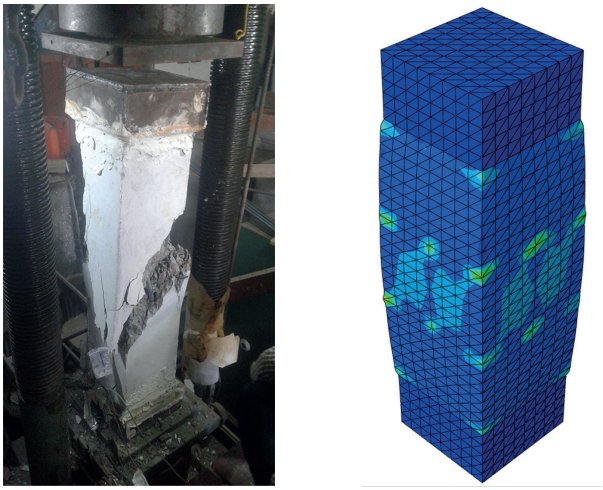

(a) (b)

Fig. 29 Modes of failure and crack survey for specimen COV-10.5: (a) experimental damage; (b) FE model plastic strain

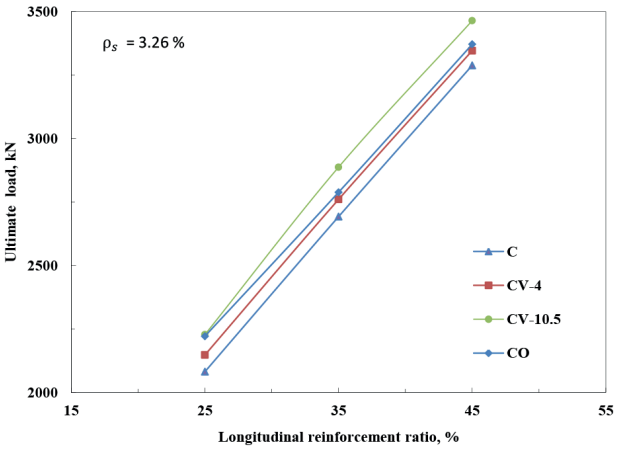

(a)

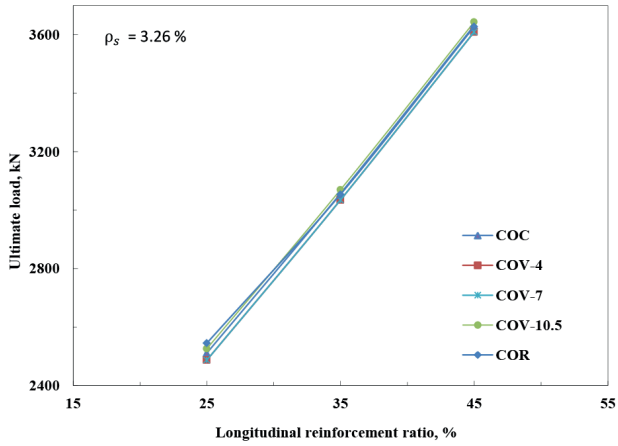

(b)

Fig. 30 Influence of concrete grade on the ultimate axial load of RC columns at longitudinal reinforcing ratio 3.26%: (a) group 1; (b) group 2

For group 1, concrete grade increased from 25 to 35 and 45 Mpa. It was observed that enhancement in axial capacity for specimen CV-10.5 was 29.6% and 55.5% respectively, while the axial capacity enhancement for column CO was 25.5% and 51.8%, respectively. In group 2, COV-10.5 achieved an increase in ultimate load of 21.5% and 44.2% by increasing concrete grade to 35 and 45 Mpa, respectively. The axial load of COR increased by 20% and 42.5% when concrete grade increased to 35 and 45 Mpa, respectively.

For group 1, at longitudinal reinforcing ratio 3.26% and concrete grade 25 MPa, the ultimate axial load of specimen CV-10.5 was 0.27% more than that of specimen CO. However, increasing concrete grade to 45 MPa, specimen CV-10.5 achieved an increase in ultimate axial load by 2.76% compared with specimen CO. In group 2, at longitudinal reinforcing ratio 3.26% and concrete grade 25 MPa, the ultimate axial load of specimen COV-10.5 was 0.75% lower than that specimen COR. However, increasing concrete grade to 45 MPa, specimen COV-10.5 achieved an increase in ultimate axial load by 0.44% compared with specimen COR. This means that the V-ties were more effective and suitable when increasing the concrete grade.

Figs. 31 and 32 present the effect of concrete grade on the ultimate load of RC columns at the longitudinal reinforcing ratio 2.57% and 1.45%, respectively. Based on these figures, it was clear that the ultimate axial loads of RC columns increased linearly by the increase in concrete grade and gave the same trend of specimens at the longitudinal reinforcing ratio 3.26%. This means that the V-ties are more effective and suitable by increasing the concrete grade compared to other traditional ties.

7.2 Longitudinal reinforcement ratio

In the present study, the influence of longitudinal reinforcing ratio was investigated by developing FE models for all specimens. Each specimen was modeled at different values of longitudinal reinforcing ratio of 1.45% (8 bars of

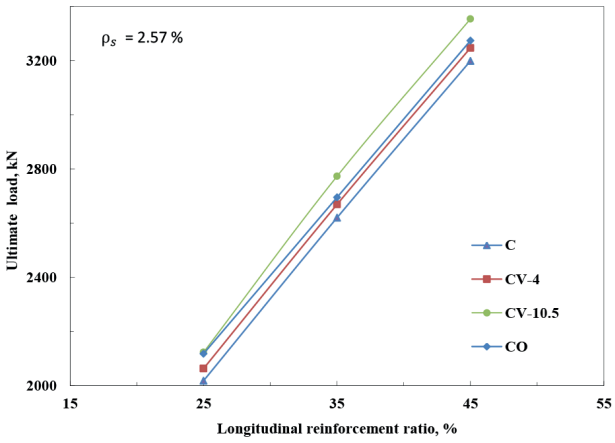

(a)

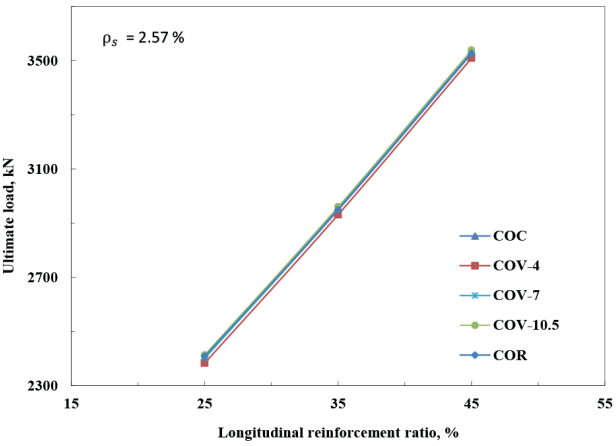

(b)

Fig. 31 Effect of concrete grade on the ultimate axial load of RC columns at longitudinal reinforcing ratio 2.57%: (a) group 1; (b) group 2

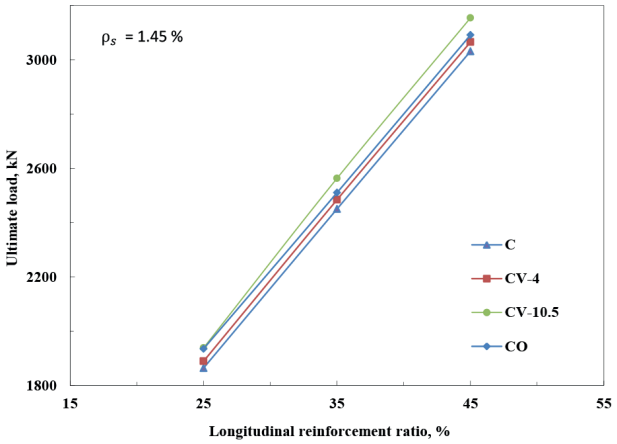

(a)

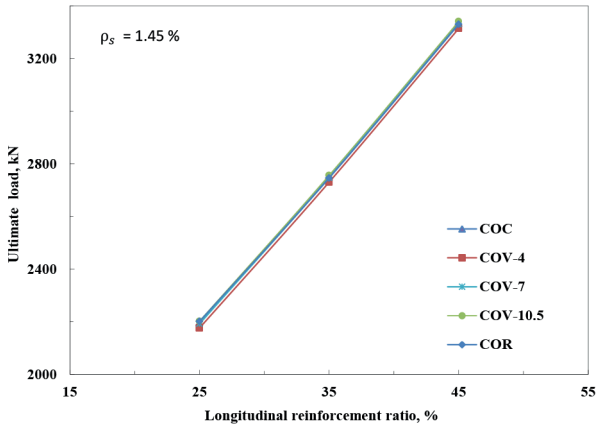

(b)

Fig. 32 Influence of concrete grade on the ultimate axial load of RC columns at longitudinal reinforcing ratio 1.45%: (a) group 1; (b) group 2

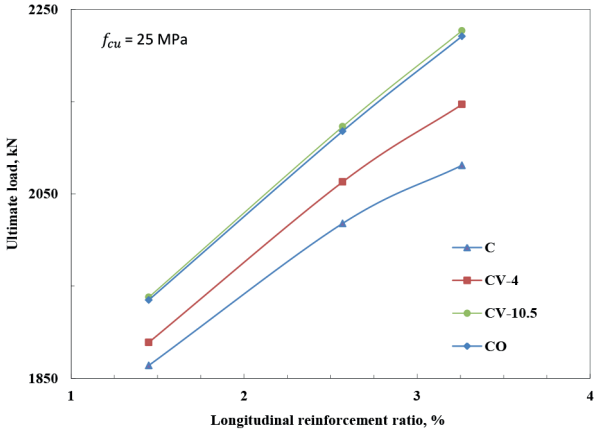

(a)

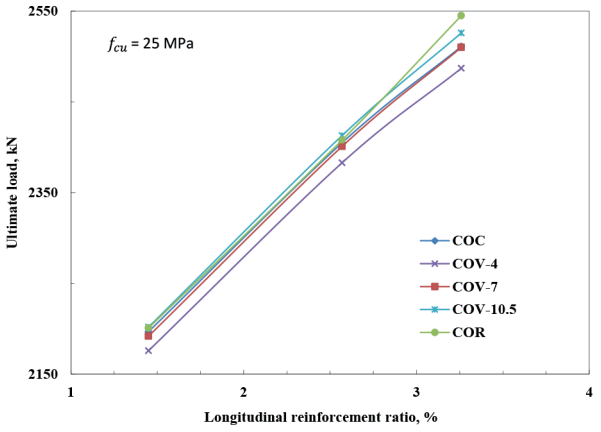

(b)

Fig. 33 Effect of longitudinal reinforcing ratio on the ultimate axial load of RC columns at concrete grade 25 MPa: (a) group 1; (b) group 2

12 mm diameter), 2.57% (8 bars of 16 mm diameter) and 3.26% (8 bars of 18 mm diameter) at different values of concrete grade 25, 35 and 45 MPa.

Fig. 33 summarizes the influence of longitudinal reinforcing ratio on the ultimate axial load of RC columns at concrete compressive strength of 25 MPa. It could be noted that the ultimate axial loads of RC columns decreased linearly by decreasing the longitudinal reinforcing ratio. It could be noted that by lowering the longitudinal reinforcing ratio, the differences in ultimate loads between V-ties columns and columns reinforced with other traditional ties were reduced. This showed that decreasing the longitudinal reinforcing ratio V-ties was more influential compared to other traditional ties.

In group 2 and at concrete grade 25 MPa, the ultimate axial load of specimen COV-10.5 was 0.75% lower than that of specimen COR at longitudinal reinforcing ratio 3.26%. However, decreasing longitudinal reinforcing ratio to 2.57% specimen COV-10.5 achieved an increase in ultimate axial load by 0.2% compared with specimen COR. This means that the V-ties are more effective and suitable when decreasing the longitudinal reinforcing ratio.

Figs. 34 and 35 present the influence of longitudinal reinforcing ratio on the ultimate load of RC columns at concrete compressive strength 35 and 45 MPa, respectively. As demonstrated in the Figs., the specimens gave almost the same trend of specimens at concrete grade 25 MPa. This means that the V-ties are more effective and suitable compared with traditional ties when decreasing the longitudinal reinforcing ratio.

The results obtained from the parametric study, showed that the enhancement in ultimate axial load of RC columns is more pronounced in V-ties than in other traditional ties by increasing concrete grade and decreasing longitudinal reinforcing ratio.

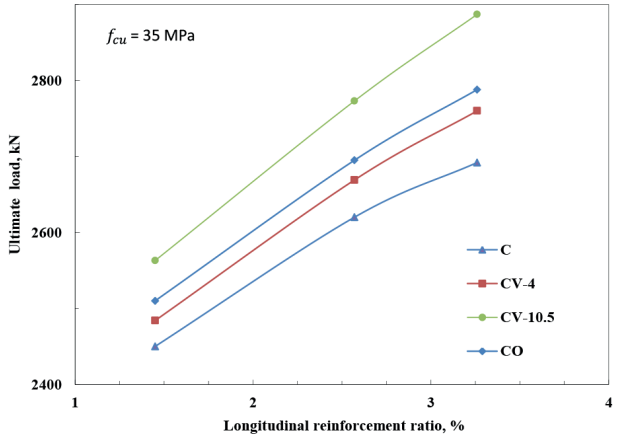

(a)

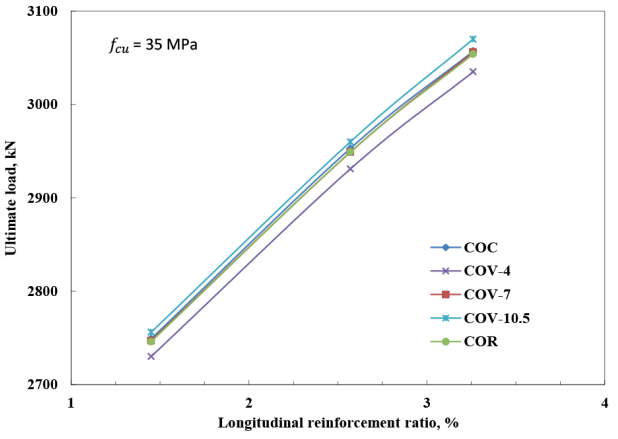

(b)

Fig. 34 Influence of longitudinal reinforcing ratio on the ultimate axial load of RC columns at concrete grade 35 MPa: (a) group 1; (b) group 2

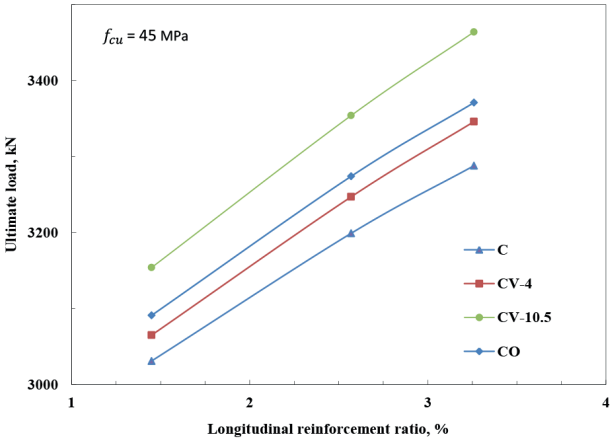

(a)

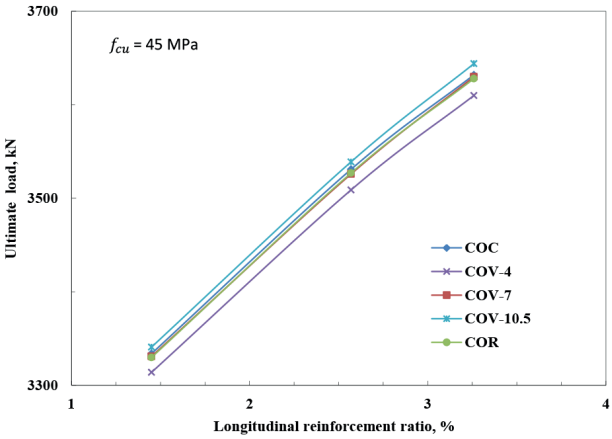

(b)

Fig. 35 Effect of longitudinal reinforcing ratio on the ultimate axial load of RC columns at concrete grade 45 MPa: (a) group 1; (b) group 2

8 Conclusions

The current paper proposed and implemented new arrangement of outer and internal transverse reinforcement for square RC short columns subjected to axial compression. The performance of RC columns improved by using V-tie techniques which was shown by comparing it with columns reinforced with traditional ties. Based on the results of the experimental and numerical investigations and according to adopted concrete dimensions, material properties, longitudinal reinforcing ratio, and tie configurations, the following conclusions could be drawn:

1. The failure modes of the test specimens proved that V-ties could be effective in providing lateral support for both corner and middle longitudinal reinforcing bars.
2. Using V-ties as transverse reinforcement for middle bars resulted in an almost similar ultimate load capacity to that obtained using traditional cross-ties. V-ties could outperform cross-ties, for leg length of 85 mm, by 1.7% increase in ultimate load capacity.
3. The effect of using V-ties instead of traditional ties on the columns' stiffness and axial strain was generally insignificant.
4. The obtained ratios of the strength gain relative to the weight of the transverse reinforcement showed that the use of V-ties is economically competitive.
5. The numerical results obtained using the proposed CDP model could provide fair agreement with the experimental results for all tested columns.
6. Enhancement in ultimate axial load of RC columns is more pronounced in V-ties than in other traditional ties by increasing concrete grade and decreasing longitudinal reinforcing ratio.
7. The results of this study highlighted the need for design codes to consider the effect of V-ties as transverse reinforcement for RC columns.

References

[1] ACI Committee 318 "Building Code Requirements for Structural Concrete (ACI 318M-19) and Commentary (ACI 318RM-19)", American Concrete Institute (ACI), Farmington Hills, MI, USA, 2019.

[2] Kim, T.-H., Lee, J.-H., Shin, H. M. "New arrangement of transverse reinforcement in rectangular solid columns", ACI Structural Journal, 116(3), pp. 207–218, 2019. https://doi.org/10.14359/51713310

[3] Yang, K.-H., Kim, W.-W. "Axial compression performance of reinforced concrete short columns with supplementary V-shaped ties", ACI Structural Journal, 113 (6), pp. 1347–1356, 2016. https://doi.org/10.14359/51689159

[4] Hwang, H.-J., Noh, J.-O., Park, H.-G. "Structural capacity of reinforced concrete columns with U-shaped transverse bars", Engineering Structures, 216, Article number: 110686, 2020. https://doi.org/10.1016/j.engstruct.2020.110686

[5] Watson, S., Zahn, F. A., Park, R. "Confining Reinforcement for Concrete Columns", Journal of Structural Engineering, 120(6), pp. 1798–1824, 1994. https://doi.org/10.1061/(ASCE)0733-9445(1994)120:6(1798)

[6] SakaiI, K., Sheikh, S. A. "What Do We Know About Confinement in Reinforced Concrete Columns? (A critical review of previous work and code provisions)", ACI Structural Journal, 86(2), pp. 192–207, 1989. https://doi.org/10.14359/2705

[7] Lukkunaprasit, P., Sittipunt, C. "Ductility Enhancement of Moderately Confined Concrete Tied Columns with Hook-Clips", ACI Structural Journal, 100(4), pp. 422–429, 2003. https://doi.org/10.14359/12650

[8] Chung, H.-S., Yang, K.-H., Lee, Y.-H., Eun, H.-C. "Strength and ductility of laterally confined concrete columns", Canadian Journal of Civil Engineering, 29(6), pp. 820–830, 2002. https://doi.org/10.1139/l02-084

[9] Dassault Systems "ABAQUS Analysis User's Manual, (6.14)", Dassault Systems Simulia Corp., Providence, RI, USA, 2014.

[10] Abdullah, A. M. "Analysis of repaired/strengthened RC structures using composite materials: Punching shear", [pdf] PhD Thesis, University of Manchester, 2010. Available at: https://www.research.manchester.ac.uk/portal/files/54505856/FULL_TEXT.PDF

[11] Lubliner, J., Oliver, J., Oller, S., Oñate, E. "A plastic-damage model for concrete", International Journal of Solids and Structures, 25(3), pp. 299–326, 1989. https://doi.org/10.1016/0020-7683(89)90050-4

[12] Genikomsou, A. S., Polak, M. A. "Finite element analysis of punching shear of concrete slabs using damaged plasticity model in ABAQUS", Engineering Structures, 98, pp. 38–48, 2015. https://doi.org/10.1016/j.engstruct.2015.04.016

[13] Wosatko, A., Winnicki, A., Polak, M. A., Pamin, J. "Role of dilatancy angle in plasticity-based models of concrete", Archives of Civil and Mechanical Engineering, 19(4), pp. 1268–1283, 2019. https://doi.org/10.1016/j.acme.2019.07.003

[14] Ali, O., Abbas, A., Khalil, E., Madkour, H. "Numerical investigation of FRP-confined short square RC columns", Construction and Building Materials, 275, Article number: 122141, 2021. https://doi.org/10.1016/j.conbuildmat.2020.122141

[15] Wahalathantri, B. L., Thambiratnam, D., Chan, T., Fawzia, S. "A Material Model for Flexural Crack Simulation in Reinforced Concrete Elements Using ABAQUS", In: Cowled, C. J. L. (ed.) Proceedings of the First International Conference on Engineering, Designing and Developing the Built Environment for Sustainable Wellbeing. Queensland University of Technology, Australia, 2011, pp. 260–264. [online] Available at: http://eprints.qut.edu.au/41712/

[16] Nayal, R., Rasheed, H. A. "Tension Stiffening Model for Concrete Beams Reinforced with Steel and FRP Bars", Journal of Materials in Civil Engineering, 18(6), pp. 831–841, 2006. https://doi.org/10.1061/(ASCE)0899-1561(2006)18:6(831)

[17] Desayi, P., Krishnan, S. "Equation for the Stress-Strain Curve of Concrete", ACI Structural Journal, 61 (3), pp. 345–350, 1964. https://doi.org/10.14359/7785

[18] Yu, T., Teng, J. G., Wong, Y. L., Dong, S. L. "Finite element modeling of confined concrete-I: Drucker–Prager type plasticity model", Engineering Structures, 32(3), pp. 665–679, 2010. https://doi.org/10.1016/j.engstruct.2009.11.014

[19] Bui, T.-T., Limam, A., Nana, W.-S.-A., Ferrier, E., Bost, M., Bui, Q.-B. "Evaluation of one-way shear behaviour of reinforced concrete slabs: experimental and numerical analysis", European Journal of Environmental and Civil Engineering, 24(2), pp. 190–216, 2017. https://doi.org/10.1080/19648189.2017.1371646

[20] Hu, H.-T., Schnobrich, W. C. "Constitutive Modeling of Concrete by Using Nonassociated Plasticity", Journal of Materials in Civil Engineering, 1(4), pp. 199–216, 1989. https://doi.org/10.1061/(ASCE)0899-1561(1989)1:4(199)

[21] Sakr, M. A., Osama, B., El Korany, T. M. "Modeling of ultra-high performance fiber reinforced concrete columns under eccentric loading", Structures, 32, pp. 2195–2210, 2021. https://doi.org/10.1016/j.istruc.2021.04.026